PHYSICS ENGINEERING

Digital lensless holographic microscopy and applications

INGENIERÍA FÍSICA

Microscopia holográfica digital sin lentes y aplicaciones

Jorge García-Sucerquía*

**Escuela de Física, Universidad Nacional de Colombia. Medellin, Colombia.*
jigarcía@unal.edu.co

(Recibido: Noviembre 26 de 2015 - Aceptado: Agosto 16 de 2016)

Resumen

En este artículo se discuten los principios y algunas aplicaciones de la microscopia holográfica digital sin lentes (MHDSL) como una herramienta para el estudio del micromundo. Se analizan los procesos de registro y reconstrucción de MHDSL para estudiar su poder de resolución lateral. Se presenta el efecto de la coherencia espacial en el estudio de una sección de la cabeza de una mosca Drosophila Melanogaster por medio de la MHDSL. Se aplica la MHDSL al estudio de sistemas coloidales dinámicos y estáticos como una prueba de la capacidad de resolución espacial micrométrica sin la necesidad del uso de lentes.

Palabras clave: *Coherencia espacial parcial, microscopía holográfica digital sin lentes, sistemas coloidales.*

Abstract

The principles and some applications of the digital lensless holographic microscopy (DLHM) to study the microworld are shown in this paper. The recording and reconstruction processes of the DLHM are analyzed to study its lateral resolution power. The effect of the spatial coherence in the study of a section of the head of a Drosophila melanogaster fly are presented. DLHM is applied to study dwynamic and static colloidal systems as a proof of the capability of achieving micrometer spatial lateral resolution without the use of lenses.

Keywords: *Colloidal systems, digital lensless holographic microscopy, spatial coherence.*

1. Introduction

The recovery of the amplitude and phase of an electromagnetic wave scattered by an object, is a unique opportunity offered by holography (Gabor, 1948, 1949, 1951). Holography is a two-steps imaging technique. In the first stage, called *recording*, the interference pattern between an object wave, that carries the information of the object, and a reference wave, whose amplitude and phase is known, is stored. From this intensity recording, named *hologram*, the complex amplitude of the object wave can be recovered, in the second stage of holography named reconstruction. While the recording process of the hologram can be modeled as a superposition in amplitude of the object and reference wave, the reconstruction process can be understood as the diffraction suffered by a known in the hologram, also understood this latter as a diffraction grating. This understanding, combined with the possibility of handling digital information of the recorded hologram (Goodman & Lawrence, 1967), opened a new spectrum of opportunities for holography and marked the genesis of what is known today as digital holography (Goodman & Lawrence, 1967; Schnars, 1994). The digital world allowed the visualization and quantification of the amplitude and phase of the reconstructed wave, it also provided holography a new set of tools which meant an additional spectrum of possibilities for the versatility that provides the digital component. For example, it was possible to remove the limitations that made Gabor's in-line architecture unattractive, reviving interest in this simple, but robust geometry for making holography (Fink et al., 1991; García-Sucerquía et al., 2006b).

The world of digital holography eliminated the need of the chemical processing the holographic plates in which interference patterns were registered, and from where the information of the object of interest was recovered. The price paid for this feature was the reduced quality of the recovered images plagued by speckle noise (García-Sucerquía et al., 2006a), and by the need to magnify the interference patterns in order to enable its recording in the digital cameras available in the market (Kreis, 2002). Off-axis geometries with maximum angle of three degrees between the reference and object (Schnars, 1994; Picart & Leval, 2008), systems using magnification of interference patterns (Cuche et al., 1999), or on-axis configurations in which the magnification of the interference pattern is accomplished by illuminating the sample with a spherical wave and propagation in free space (Barton, 1988; Fink et al., 1991; Kreuzer et al., 1995; García-Sucerquía et al., 2006b), were the option to make the digital approach to holography a reality. This latter option was the genesis of a lensless microscopy technique, initially known by the name of digital in-line holographic microscopy (García-Sucerquía et al., 2006b) and now known as digital lensless holographic microscopy (DLHM). This article summaries the principles and some of the applications that DLHM offers in the study of the microworld.

2. Method

This section describes the basics of DLHM and its resolution power from an wave analysis of the problem.

2.1 Fundamentals of DLHM

DLHM is a lensless methodology of imaging in two stages: i) recording and ii) reconstruction (García-Sucerquía et al., 2006b; Jericho & Kreuzer, 2011). To accomplish the recording the sample is illuminated with spherical waves to ensure the magnification of the diffraction pattern by the free space propagation and make possible the recording in a commercial digital camera. To generate the spherical waves, a monochromatic light source, usually a laser with wavelength λ, is focused down onto a pinhole with a diameter of the order of λ. In this way, the sample located at a z distance from the pinhole, is illuminated by highly coherent spherical waves. The portion of the waves weakly scattered by the sample, known as *object wave*, interferes on the surface of the digital sensor, either a camera CMOS (complementary metal-oxide semiconductor) or CCD (charge-coupled device), with the portion of the waves not scattered, called *reference wave*.

The digital sensor is positioned so that its center is at a distance L from the pinhole. The recorded intensity by the digital sensor, called in-line hologram, it is transferred to a PC for its further processing. In Figure 1 the recording pro-cess of DLHM is illustrated.

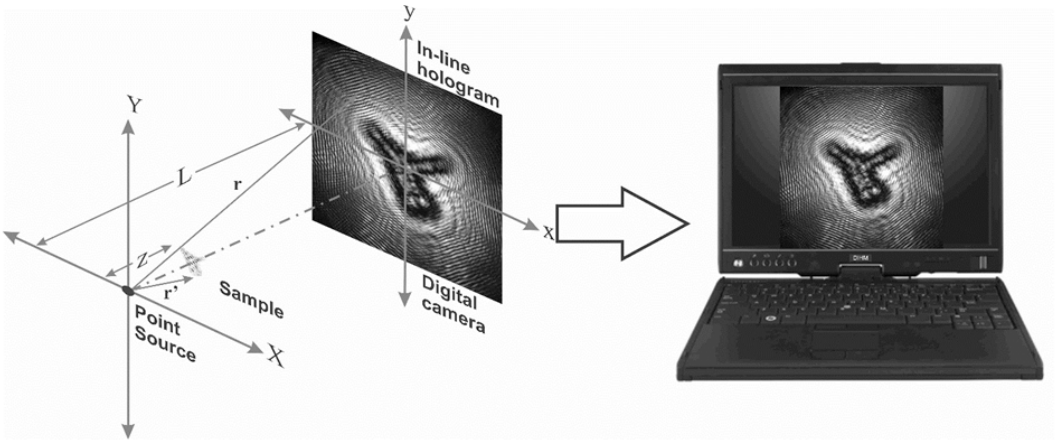

Figure 1. *Recording stage in digital lensless holographic microscopy (DLHM).*

The in-line hologram can be written as the superposition in amplitude of the object wave and the reference wave U_{ref} **(r)**

$$I(\mathbf{r}) = \left|U_{scat}(\mathbf{r})\right|^2 + \left|U_{ref}(\mathbf{r})\right|^2 + \left[U_{scat}(\mathbf{r})U^*_{ref}(\mathbf{r}) + U^*_{scat}(\mathbf{r})U_{ref}(\mathbf{r})\right]. \quad (1)$$

According to equation (1), the intensity recorded by th e digital camera includes the terms of the zero diffraction order $\left|U_{scat}(\mathbf{r})\right|^2 + \left|U_{ref}(\mathbf{r})\right|^2$, which made impractical Gabor's invention (Gabor, 1948). DLHM overcomes this di-fficulty by a pixel wise subtracting the irradiance of the reference wave, corresponding to the intensity recorded in the DLHM without the sample, from the intensity presented in equation (1). If additionally it is considered that the intensity of the wave scattered by the object is negligible, a new hologram, called *contrast hologram* with the following form is obtained:

$$\tilde{I}(\mathbf{r}) = \left[U_{scat}(\mathbf{r})U^*_{ref}(\mathbf{r}) + U^*_{scat}(\mathbf{r})U_{ref}(\mathbf{r})\right]. \quad (2)$$

This intensity distribution contains information about the object and reference wave in their form of twin images (Goodman, 2005), which do not present any problem in the process of reconstructing contrast holograms, as it has been shown in several publications (García-Sucerquía et al., 2006b; Jericho & Kreuzer, 2011; García-Sucerquía, 2013).

In the reconstruction stage, the object wave which carries the sample information is retrieved by numerical calculation of the diffraction process that the reference wave undergoes when it illuminates the contrast hologram. Because in DLHM the reference wave is spherical, this process can be described mathematically by the Kirchhoff-Helmholtz transform (Barton, 1988; García-Sucerquía et al., 2006b; Jericho & Kreuzer, 2011):

$$U(\mathbf{r}') = \int_{\sigma} \tilde{I}(\mathbf{r}) \exp\left[ik\left(\frac{\mathbf{r}'\cdot\mathbf{r}}{|\mathbf{r}|}\right)\right] d^2r \quad (3)$$

In equation (3) the integral extends over the surface of th e screen σ, camera CCD or CMOS, with coordinates $\mathbf{r} = (x,y,L)$, $k = 2\pi/\lambda$ is the wavenumber; $\tilde{I}(\mathbf{r})$ is the contrast hologram; and $\mathbf{r} = (x',y',z_r)$ are the coordinates in the plane of reconstruction. $U(\mathbf{r}')$ is a complex quantity that can be computed at different distances of reconstruction z_r from the pinhole; this option allows the retrieving the three-dimensional information of the sample o equivalently the wave scattered by the sample in different planes. This operation is completely performed numerically by processing a two-dimensional contrast hologram

with M x N pixels of DLHM. The contrast hologram is interpolated in a spherical type grid with pixels with $\Delta x"$,$\Delta y"$ size. A new modified hologram $\tilde{I}"(m\Delta x", n\Delta y")$, which accounts for the propagation distance z_r, is introduced in the discretized version of equation (3) to produce (Jericho & Kreuzer, 2011;

$$U(s\Delta x', t\Delta y', z_r) = \Delta x"\,\Delta y" \exp\left[ik \frac{\left(s^2 \Delta x"\,\Delta x' + t^2 \Delta y"\,\Delta y'\right)}{2L} \right] \sum_{m=-M/2}^{(M/2)-1} \sum_{n=-N/2}^{(N/2)-1} \tilde{I}"(m\Delta x", n\Delta y") \times \exp\left[ik \frac{\left(m^2 \Delta x"\,\Delta x' + n^2 \Delta y"\,\Delta y'\right)}{2L} \right] \times \exp\left[-ik \frac{\left((s-m)^2 \Delta x"\,\Delta x' + (t-n)^2 \Delta y"\,\Delta y'\right)}{2L} \right] \quad (4)$$

According with equation (4), the complex amplitude of the object wave can be computed as circular convolution by means of three fast Fourier transforms. In equation (4) the size of the coordinates of the reconstruction plane can be chosen with no dependence of the reconstruction distance, the wavelength and the size of the hologram. This feature the re construction algorithm, is essential in DLHM to adjust the size of the recording and reconstruction to the magnification produced by the spherical illumination of the sample. The reconstruction process applied to the hologram sent to the computer in Figure 1 produces the image shown in Figure 2 (A). The profile along the straight line drawn over the reconstruction image in panel (A) it is shown in panel (B). From this profile one can observed that DLHM can reach spatial resolution in the micrometer range, with no need of lenses at all. The quality of the reconstructed image allows the clear visualization of the hexagonal packing of the polystyrene spheres of 1.09μm in diameter that were utilized in this experiment.

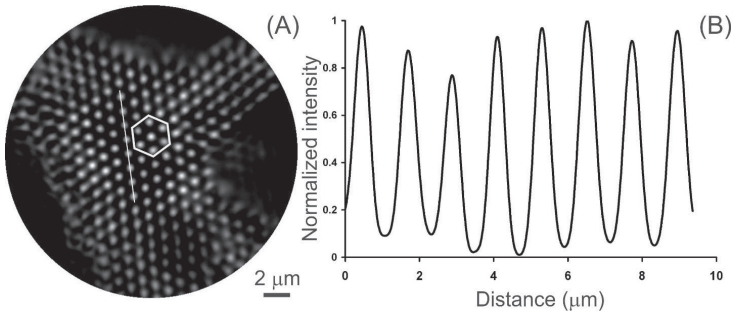

Figure 2. *Reconstruction (A) obtained from the contrast hologram produced from the in-line hologram illustrated in Figure 1. Profile (B) along the straight line in panel (A).*

2.2 Lateral resolution in DLHM

In this section, a criterion based on the geometrical parameters of the microscope to evaluate the lateral resolution of DLHM is derived; the criterion is demonstrated by means of computer modeling. For simplicity it is considered that the digital screen is placed perpendicular to the optical axis, which links the point source (pinhole) and the center of the digital camera. The object wave is produced by two point objects symmetrically located with respect to the optical axis and connected with a straight line parallel to the digital camera; if each point object is denoted by a position vector it can be said that $|\mathbf{r}_1| = |\mathbf{r}_2|$. The contrast hologram can be written as:

$$\tilde{I}(\mathbf{r}) = 4\frac{U_0 U_1}{r|\mathbf{r}-\mathbf{r}_1|}\cos\left[\frac{\pi}{\lambda}\left(2r-|\mathbf{r}-\mathbf{r}_1|-|\mathbf{r}-\mathbf{r}_2|\right)\right]\cos\left[\frac{\pi}{\lambda}\left(|\mathbf{r}-\mathbf{r}_1|-|\mathbf{r}-\mathbf{r}_2|\right)\right] \quad (5)$$

The second cosine term produces a modulation of the hologram reaching its maximum when its argument equals to 2πn, with n an integer. To recover the information stored in the contrast hologram, it is need to guarantee that at least the first zero and the first maximum of the diffraction patterns is recorded in the digital camera. Under the former premise, it can be shown that two points can be laterally resolved if it is fulfilled the condition (García-Sucerquía *et al.*, 2006b):

$$|\mathbf{r}_1-\mathbf{r}_2| \geq \frac{\lambda}{2NA} \quad (6)$$

with *NA* the numerical aperture of the microscope defined as $NA = W/2\left(\sqrt{(W/2)^2+L^2}\right)$, with W the width of the digital camera.

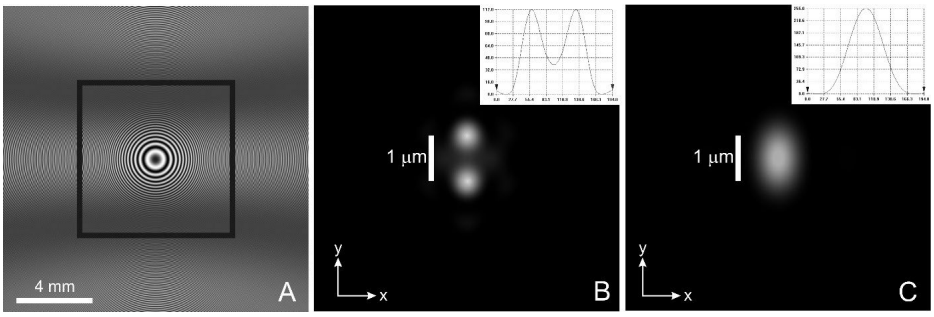

Figure 3. *Test of lateral resolution. A: hologram of two point close to the optical axis 1µm apart. Hologram modeled with a blue laser λ=473nm and 0.5 numerical aperture 0.5 (0.28 for the interior square). B: reconstruction for the whole hologram where sub-micrometer resolution is shown. C: reconstruction of the inner part of the hologram; the loss of lateral resolution is evident.*

In Figure 3A is shown a modeled hologram produced by two points 1µm apart. The hologram was recorded with a blue laser and 0.5 numerical aperture. The reconstruction of the hologram should exhibit two separated points, as it is clearly presented in Figure 3B. If now the numerical aperture is reduced, namely it is only considered the inner part of the hologram in Figure 3A reducing the numerical aperture to 0.28, the micrometer sized spatial resolution is no longer reach, as illustrated in Figure 3C.

3. Results and discussion

In this section two applications of DLHM are presented. The use of light sources with partial spatial coherence is shown to image a biological specimen and static and dynamic colloidal systems.

3.1 DLHM with light sources with partial spatial coherence to study biological samples

To implement DLHM with a light source which has partial spatial coherence, the light from a superbright LED was focused down onto the surface of a pinhole with diameter d_p. The incoherent blue LED has a mean wavelength $\bar{\lambda}$=450 nm and a FWHM of 25 nm which allows the recording of in-line holograms of samples up to 8 µm thick. The partial coherence of the light over the sample is determined by the Van Cittert-Zernike theorem (Born & Wolf, 2005) what stablish that the diameter of the area almost coherently illuminated is given by $D_{coh} = 0.32\bar{\lambda}z/d_p$, where z is the distance from the pinhole to the sample. In this way, for a fixed pinhole-sample distance the spatial coherence of the light source can be changed by the simple variation of the pinhole diameter d_p. A complementary discussion on the effect of the spatial partial coherence in DLHM can be read for instance in Gopinathan et al. (2008).

To make experiments with spatial partial coherence in DLHM a section of the head of a fruit fly prepared with Bodian´s method (Bodian, 1936) was imaged. The simple is of the order of 900 µm in width and has thickness of 5 µm. The panels in Figure 4 show the reconstructed images as the spatial coherence of

the illuminating light is changed over the sample. The diameter that is almost coherently illuminated (D_{coh}) is changed from 6.2 μm for panel A to 115 μm for panel E, see figure caption for the other parameters; panel F is the reconstructed image as the hologram is recorded with a completely coherent light source. This latter image was obtained by means of a violet laser λ=405 nm illuminating a pinhole 0.5 μm in diameter. For panels A and B, the low spatial coherence of the light source leads to reconstructed images where the overall shape of the simple is visible, but few details of the internal structure are seen, namely, the spatial resolution of the microscope has been reduced due to the widening of the point spread function of it (Gopinathan et al., 2008). As the spatial coherence is increased over the plane of the simple, it can be seen a larger number of the internal details of the specimen and the edges of the simple are sharper, see panels C, D y E. Panels D, E and F show a comparable spatial resolution of the spatial partial coherent DLHM with that of fully coherent DLHM, however the former shows a better signal-to-noise ratio (SNR) than the fully spatial coherence DLHM.

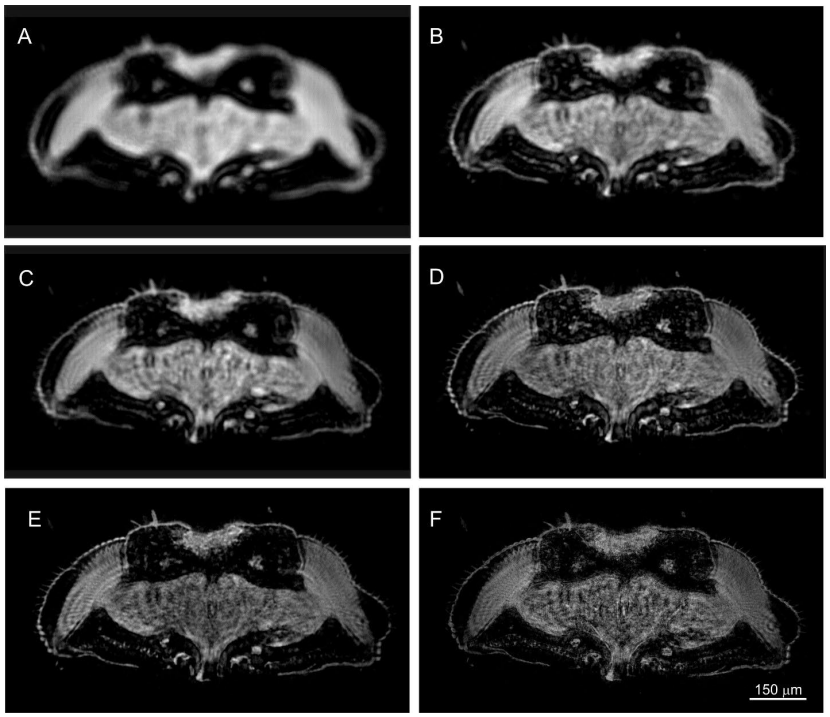

Figure 4. *Effect of spatial coherence in DLHM. The diameter of the area that is almost coherently illuminated is =6.2 μm, 9.4μm, 20.1μm, 40.8μm and 115μm for figures A, B, C, D and E for pinhole diameters dp = 30μm, 20μm, 10μm, 5μm and 2 μm, in that order; the mean wavelenght is =450 nm. The image in figure F corresponds is the reconstructed image for fully coherent illumination and wavelength λ=405 nm. For all the experiments the numerical aperture was 0.41 and the pinhole-to-sample distance was varied from z = 400 to 900 μm.*

3.2 Study of dynamic and static colloidal systems

One of the fields of great application of DLHM is the study of colloidal systems, both dynamic and static. To perform this study, 20μl of a solution of polystyrene spheres 800nm in diameter 20%vol were diluted in distilled water over a cover slide previously prepared. The continue observation of the drying process of the solution allows the recovering of information of process like nucleation, aggregation and adhesion of the spheres to the substrate. The frame in Figure 5 was extracted from a video which was monitored the drying process of the solution above described. The wavy form of gray color, is an indication of the dewetting front over

the substrate. The circular regions show groups of spheres which also contain some debris trapped in the water. For this particular experiment an average speed of 140μm/s was measure for the dewetting front in the left-side to right-side (Alvarez-Palacio & García-Sucerquía, 2010).

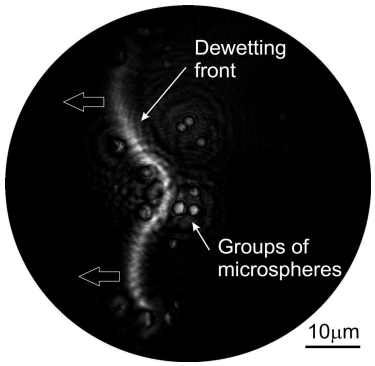

Figure 5. *DLHM to study dynamic colloidal systems. Frame extracted from a video that records the dewetting process of a colloidal suspension of polystyrene in distilled water. The arrows on the profile indicate the direction of the dewetting front.*

Once the water has been completely evaporated, it is possible to visualize the shape of the self-arrangement of the spheres over the surface of the substrate. In Figure 6 (A) it is shown the reconstructed image corresponding to a monolayer of spheres of polystyrene 800nm in diameter. In this experiment a 532nm laser was focused down over a pinhole of 500nm of diameter. The digital camera was placed such that the numerical aperture of the DLHM was 0.6 (García-Sucerquía et al., 2006b). That numerical aperture and illuminating wavelength lead to a theoretical spatial resolution for the DLHM of $\Delta r \approx \lambda/2NA = 444$nm. Such spatial resolution is enough to have a clear visualization of groups of the spheres, in the same way makes possible the identification of the hexagonal packing that follows the spheres. The spatial resolution of DLHM has evolved up to the level that defect and dislocations in the structure of the arrangement of the spheres can be identified (García-Sucerquía et al., 2008). In addition to the study of the monolayers in the real space, DLHM allows the study of the monolayers in the Fourier space. Figure 6 (B) shows

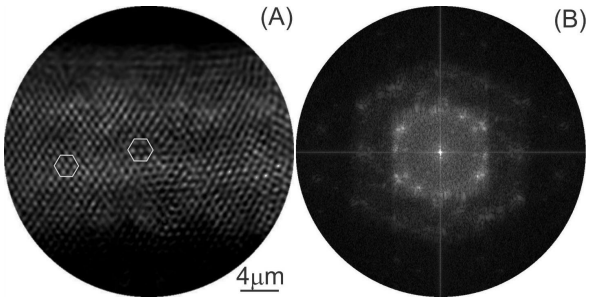

Figure 6. *DLHM utilized to study colloidal crystals. (A) Reconstruction of a hologram recorded for a monolayer of polystyrene spheres 800nm in diameter. (B) Fourier transform of the image in panel (A). The hexagonal packing of the spheres highlighted in panel (A) is verified with the Fourier transform in panel (B).*

the Fourier transform of the image in panel (A). In this transform, the hexagonal packing that follows the spheres is clearly verified. A complete and fully detailed description of the use of DLHM to study dynamic and static colloidal systems can be read in (Alvarez-Palacio & García-Sucerquía, 2010).

4. Conclusions

The fundamentals of digital lensless holographic microscopy (DLHM) and some applications to study micrometer sized samples were shown. A description of the recording and reconstruction processes of in-line digital holograms is also presented. For the reconstruction stage, it is presented a method of reconstruction with variable magnification for making possible the recovering of details in the micrometer sized scale of the simple under study.

The spatial resolution of DLHM and the effects of the partial spatial coherence in the performance of DLHM have been also presented. The use of DLHM in the study of dynamic and static colloidal systems has been presented. The illustrated results invite to use DLHM in diverse fields of research and technology. Micrometer sized spatial resolution with the use of no lenses and utilizing LED light sources, set the DLHM as a promising method to develop portable microscopes.

5. Acknowledgments

The author thanks to Universidad Nacional de Colombia, through the Programa de Internacionalización del Co-nocimiento and the program Jóvenes Investigadores de Colciencias-Universidad Nacional de Colombia code Hermes 28751.

6. References

Alvarez-Palacio, D.C., & García-Sucerquía, J. (2010). Lensless microscopy technique for static and dynamic colloidal systems. *Journal of Colloid and Interface Science* 349 (2), 637-640.

Barton, J.J. (1988). Photoelectron Holography. *Physical Review Letters* 61 (12), 1356-1359.

Bodian, D. (1936). A new method for staining nerve fibers and nerve endings in mounted paraffin sections. *The Anatomical Record* 65 (1), 89-97.

Born, M., & Wolf, E. (2005). *Principles of Optics.* 7th ed. Cambridge-UK: Cambridge University Press.

Cuche, E., Bevilacqua, F., & Depeursinge, C. (1999). Digital holography for quantitative phase-contrast imaging. *Opt. Lett*. 24 (5), 291-293.

Fink, H.-W., Schmid, H., Kreuzer, H., & Wierzbicki, A. (1991). Atomic resolution in lensless low-energy electron holography. *Physical Review Letters* 67 (12), 1543-1546.

Gabor, D. (1948). A new microscopic principle. *Nature* 161 (4098), 777-778.

Gabor, D. (1949). Microscopy by reconstructed wave-fronts. *Proc. R. Soc. London A* 197 (1051), 454.

Gabor, D. (1951). Microscopy by reconstructed wave fronts: II. *Proc. Phys. Soc. London* B 64 (6), 449.

García-Sucerquía, J. (2013). Noise reduction in digital lensless holographic microscopy by engineering the light from a light-emitting diode. *Applied Optics* 52 (1), A232-A239.

García-Sucerquía, J., Alvarez-Palacio, D.C., & Kreuzer, H.J. (2008). High resolution Talbot self-imaging applied to structural characterization of self-assembled monolayers of microspheres. *Appl. Opt*. 47 (26), 4723-4728.

García-Sucerquía, J., Ramírez, J.H., Castañeda, R., Herrera-Ramírez, J., & Castañeda, R. (2006a). Incoherent recovering of the spatial resolution in digital holography. *Optics Communications* 260 (1), 62-67.

García-Sucerquía, J., Trujillo, C., & Restrepo Agudelo, J. (2014). *Microscopio holográfico digital sin lentes (MHDSL) y método para visualizar muestras*. Patent Filed 14258943 0 0.

García-Sucerquía, J., Xu, W., Jericho, S.K., Klages, P., Jericho, M.H., & Kreuzer, H.J. (2006b). Digital in-line holographic microscopy. *Appl. Opt*. 45 (5), 836-850.

Goodman, J.W. (2005). *Introduction to Fourier Optics*. Greenwood Village: Roberst & Company Publishers.

Goodman, J.W., & Lawrence, R.W. (1967). Digital image formation from electronically detected holograms. *Applied Physics Letters* 11 (3), 77-79.

Gopinathan, U., Pedrini, G., & Osten, W. (2008). Coherence effects in digital in-line holographic microscopy. J. *Opt. Soc. Am. A* 25 (10), 2459-2466.

Jericho, M.H., & Kreuzer, H.J. (2011). Point Source Digital In-line Holographic Microscopy. In: P. Ferraro, A. Wax and Z. Zalevvsky, eds., Coherent Light Microscopy. Springer-Verlag Berlin Heidelberg, (Chapter 1).

Kreis, T.M. (2002). Frequency analysis of digital holography. *Optical Engineering* 41 (4), 771-778.

Kreuzer, H.J., Fink, H.W., Schmid, H., & Bonev, S. (1995). Holography of holes, with electrons and photons. *Journal of Microscopy* 178 (3), 191-197.

Picart, P., & Leval, J. (2008). General theoretical formulation of image formation in digital Fresnel holography: erratum. J. *Opt. Soc. Am. A* 26 (2), 244.

Schnars, U. (1994). Direct phase determination in hologram interferometry with use of digitally recorded holograms. J. *Opt. Soc. Am. A* 11 (7), 2011-2015.